Supporting Information for:

Title: Active droplets through enzyme-free, dynamic phosphorylation

Authors: Simone Poprawa,[1] Michele Stasi,[1] Monika Wenisch,[1] Brigitte A. K. Kriebisch,[1] Judit Sastre,[1] Job Boekhoven[1]

Affiliations:

[1] Department of Bioscience, Technical University of Munich, Lichtenbergstrasse 4, 85748 Garching, Germany

Materials and methods

Materials. All chemicals were purchased from Sigma-Aldrich, VWR, or TCI Europe and used without further purification. General solvents were purchased from Sigma Aldrich in analytical or synthesis grade and used without further purification. Dimethylsulfoxide-D6 in glass ampoules was purchased from Sigma-Aldrich. Sylgard 184 silicon elastomere were all purchased from Sigma-Aldrich. 3M™ Novec™ 7500 oil (dOil) and 2% fluorosurfactant (dSURF) were purchased from Fluigent. The peptide NH_2-R_{30}-OH (R_{30}) was purchased from CASLO Aps.

Synthesis of potassium monoamidophosphate. DAP was synthesized, as previously reported by Ying-Fei Wei and Harry R. Matthews.[1] 371 mg MAP were obtained (2.75 mmol, 31 %). It was characterized by ^{31}P-NMR and elemental analysis.

^{31}P-NMR (D_2O, pH = 6.5, 500 MHz): δ -3.88

Elemental analysis:

theoretical values: H: 2.24%; N: 10.37%; K: 28.94%; O: 35.53%; P: 22.93%

measured values: H: 2.29%; N: 9.94%; K: 29.3%; P: 21.81%.

Synthesis of Diamidophosphate. DAP was synthesized as previously reported by Krishnamurthy et al.[2] It was characterized by ^{31}P-NMR and elemental analysis.

^{31}P-NMR (D_2O, pH = 6.5, 500 MHz): δ 12.33

Elemental analysis:

theoretical values: H: 3.42%; N: 23.74%; Na: 19.48%; O: 27.12%; P: 26.25%

measured values: H: 3.62%; N: 21.06%; P: 23.69%.

Manual solid-phase peptide synthesis under controlled heating. All peptides were synthesized on a 0.5 mmol scale. Glycine preloaded Wang resin (0.5 mmol, 0.69 mmol g^{-1} loading) was used to synthesize Ac-GHG-OH, aspartic acid preloaded Wang resin (0.5 mmol, 0.67 mmol g^{-1} loading) for Ac-Y'DHDD-OH and rink amide resin (0.5 mmol, 0.29 mmol g^{-1} loading) for Ac-Y'DHDD-NH_2. The reaction vessel was connected to a nitrogen line, and the waste flask was connected to a water pump. The resin was swelled in DMF with medium nitrogen bubbling for 20 min at room temperature. The peptide synthesis was performed at 68 °C.

Before each coupling step, the *N*-terminal Fmoc-protecting group was cleaved using 10-30 mL of a 5% (w/v) solution of piperazine in DMF (for D-containing peptides, an additional 0.2 M HOBt was added). The reaction mixture was stirred with an N_2 stream for 1 minute and 5 min. The deprotecting solution was removed, and the resin was washed with DMF. For each coupling, 3 eq. of amino acid were used together with 2.8 eq. of HCTU and 6 eq. of DIPEA. HCTU and DIPEA were added to the amino acid and vortexed until dissolved. The coupling solution was added to the resin and stirred with an N_2 stream for 6 min. After the coupling, the solution was drained, and the resin was washed with DMF. The deprotection, washing, coupling, and washing cycle was carried out for each amino acid. After the last coupling, the peptide was acetyl end-capped at room temperature. Therefore, a final deprotection was conducted; the resin was washed at room temperature, and 6 eq. of acetic anhydride and 6 eq. of DIPEA in DMF solution were added to the resin and stirred with N_2 stream for 10 min at RT. The resin was washed with DMF and DCM. A cleavage solution consisting of 2.5 % MQ-water, 2.5 % TIPS, and 95 % TFA was prepared to cleave the peptide from the resin. It was added to the resin and agitated for two hours at RT. The cleavage solution was collected by filtration, and the resin was washed with DCM. The solvents were removed by co-distillation under reduced pressure using a rotary evaporator (Hei-VAP Core, VWR). The crude peptides were dissolved in H_2O:ACN (70:30) purified using a reversed-phase preparative HPLC (Thermo Fisher Dionex Ultimate 3000, Hypersil Gold 250 × 4.8 mm, Thermo ScientificTM DionexTM ChromelonTM Chromatography Data System for Ac-GHG-OH; RP-HPLC on an Agilent 1260 Infinity ll setup, Agilent InfinityLab ZORBAX SB-C_{18} column 250 mm x 21.2 mm, 5 µm particle size for Ac-Y'DHDD-OH/-NH_2). A linear gradient composed as follows was used for the purification, and the different fractions were collected at 220 nm (Ac-GHG-OH) or 235 nm (Ac-Y'DHDD-OH/-NH_2).

HPLC gradient for the purification of Ac-GHG-OH.

Time [min]	Flow rate [mL/min]	H_20	ACN
0	20	95	5
5	20	80	20
7	20	2	98
12	20	2	98
13	20	95	5
15	20	95	5

HPLC gradient for the purification of Ac-Y(OMe)DHDD-OH/-NH_2.

Time [min]	Flow rate [mL/min]	H_20	ACN
0	20	85	15
2	20	85	15
21	20	60	40
22	20	5	95
26	20	5	95
27.5	20	85	15
30	20	85	15

All peptides were lyophilized (Christ Freeze Dryer Alpha 2-4 LDplus, VWR) and stored at -20 °C. They were characterized by electrospray ionization mass spectrometry (ESI-MS, Thermo Scientific, LCQ Fleet ION Trap Mass Spectrometer) in positive or in negative mode (Supplementary Table S5), analytical HPLC (Vanquish DUO HPLC system (Chromeleon software version 7.2.10 ES) with a Hypersil-Gold, reversed-phase C_{18} column (particle size: 3 µm, length: 100 mm, ID: 2.1 mm), eluted with a gradient of 0.1% TFA H_2O:ACN for Ac-GHG-OH; Vanquish SINGLE HPLC system (Chromeleon 7 Data System Software Version 7.3.1) with EC 150/4 NUCLEODUR C_{18} Pyrmid, 3 µm (particle size: 3 µm, length: 150 mm, ID: 4

mm), Machery-Nagel; eluted with a gradient TEAA 25 mM and ACN:TEAA 25 mM 25:75 at 30 °C) detected at 220 nm and ^{1}H NMR (Figure S1 – S3).

HPLC gradient for Ac-GHG-OH.

Time [min]	Flow rate [mL/min]	H_20	ACN
0	0.4	98	2
15	0.4	2	98
16	0.4	2	98
17	0.4	98	2
20	0.4	98	2

HPLC gradient for the purification of Ac-Y(OMe)DHDD-OH/-NH_2.

Time [min]	Flow rate [mL/min]	TEAA 20 mM	ACN:TEAA 25:75
0	0.75	80	20
4	0.75	80	20
17	0.75	40	60
18	0.75	5	95
20	0.75	5	95
22	0.75	80	20
30	0.75	80	20

Characterization of the precursors.

Ac-GHG-OH	Mass calculated [g/mol]	311.12
	Mass observed [g/mol]	312.12 $[M+H]^+$
	Retention time [min]	1.19
Ac-Y(OMe)DHDD-OH	Mass calculated [g/mol]	719.24
	Mass observed [g/mol]	718.25 $[M-H]^-$

	Retention time [min]	14.0
Ac-Y(OMe)DHDD-NH_2	Mass calculated [g/mol]	718.26
	Mass observed [g/mol]	717.47 $[M-H]^-$
	Retention time [min]	11.8 (Calibration factor = 14.093)

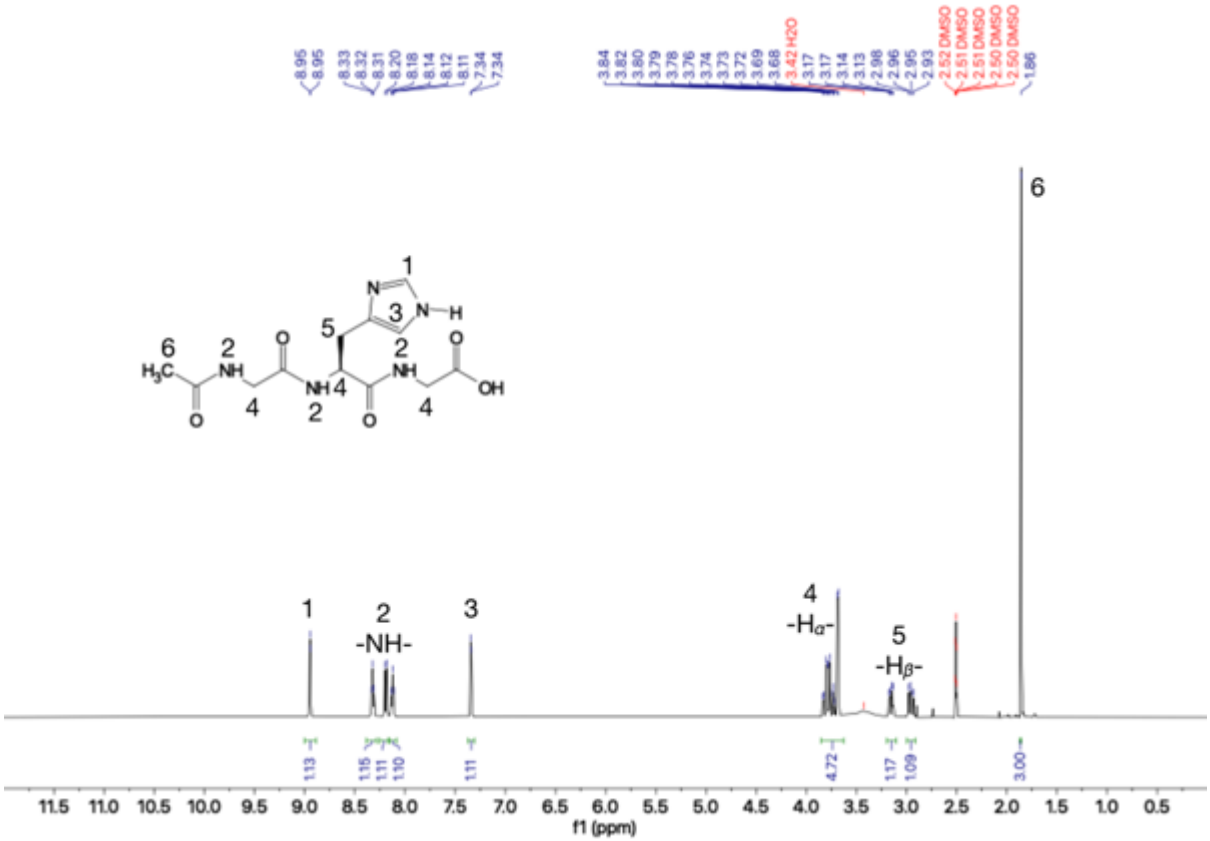

[1]H-NMR spectrum of Ac-GHG-OH.

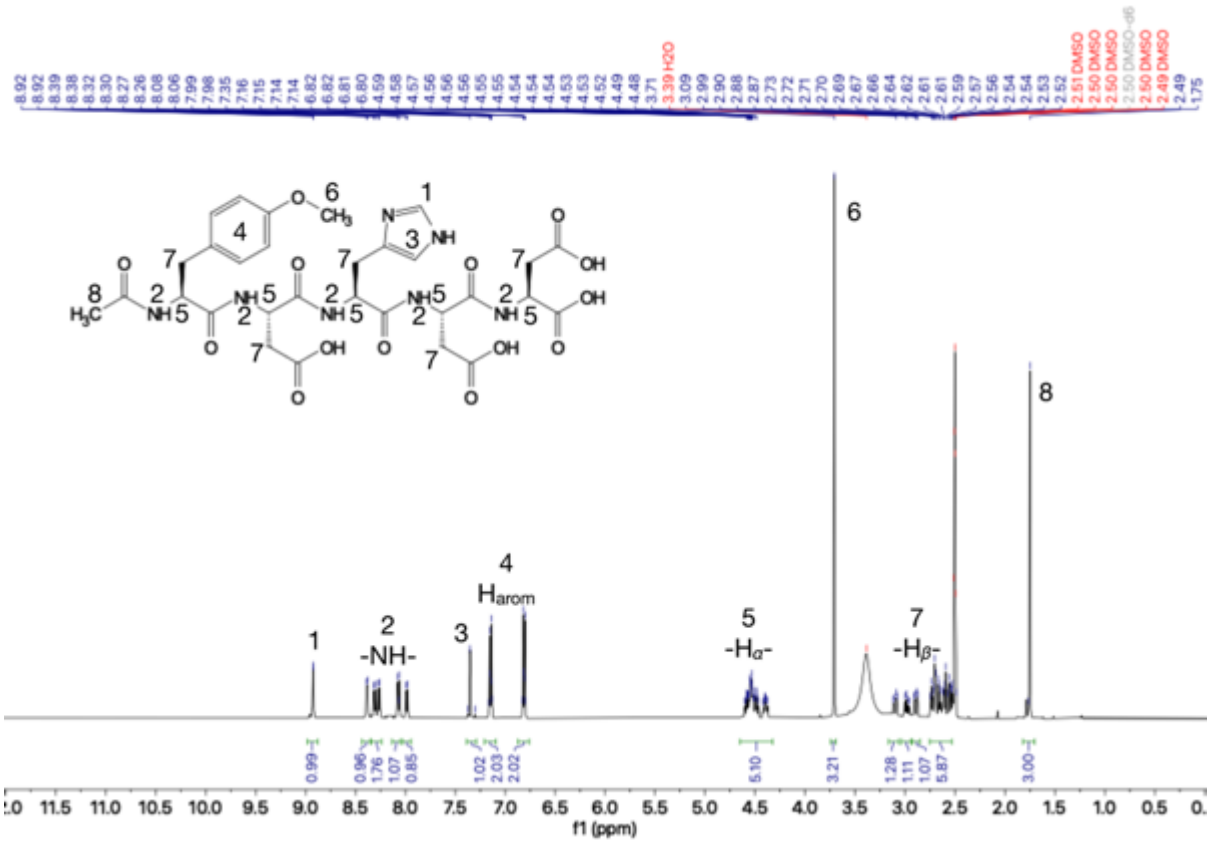

[1]H-NMR spectrum of Ac-Y(OMe)DHDD-OH.

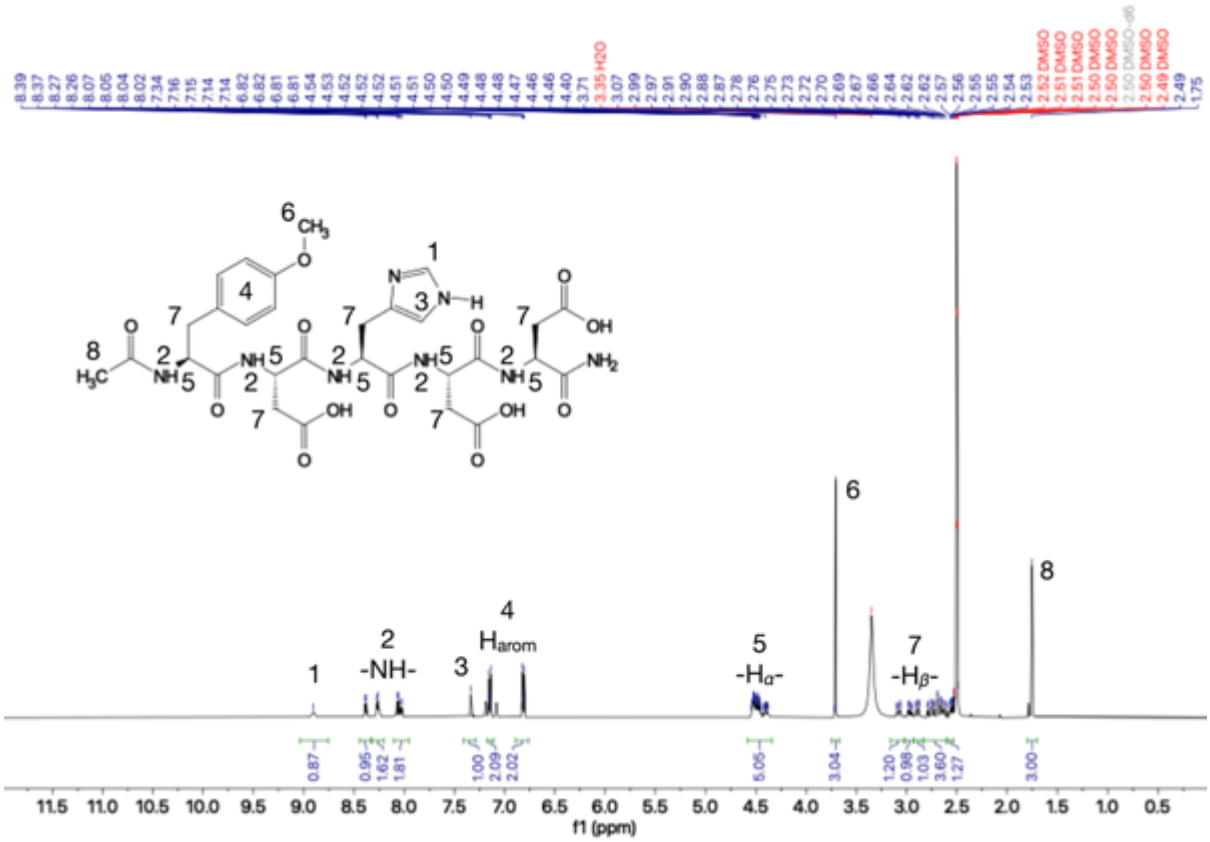

^{1}H-NMR spectrum of Ac-Y(OMe)DHDD-NH_2.

Fluorescent labeling of R30 with Cy5

For the labeling of R30 with Cy5, the protocol “Amersham CyDye mono-reactive NHS Esters - Reagents for the labeling of biological compounds with Cy monofunctional dyes - Product Booklet” published by cytiva was adapted. A solution of 1 mg Cy5-NHS ester in 50 µL DMF was prepared, adding 1 mL of a 50 mM $NaHCO_3$ buffered 62 µM R30 solution. The reaction mixture was stirred for 24 hours at room temperature. To purify the labeled peptide, it was dialyzed (Thermo scientific Slide-A-Lyzer Dialysis Cassette, 2000MWCO, 2.0 -12 mM capacity) against 2.5 mL water (12 h and 24 h) and lyophilized afterward. A degree of labeling of 0.2609 by applying *Lambert-Beer*’s law with an absorbance at 650 nm was obtained. The extinction coefficient of Cy5 is 250000 M^{-1} cm^{-1}.

Methods.

General sample preparation. MES and MOPS buffers were prepared by dissolving MES hydrate or MOPS in MQ-water (11% D_2O) to give a 500 mM solution. 5M NaOH was added to adjust the final pH of 5.5, 6.5 for MES, and 7.5 for MOPS.

Sample preparation for kinetic analysis. Stock solutions of the precursor (100 mM His, Arg, Lys, Ser, Cys, Asp, Ac-GHG-OH) were prepared in 500 mM MES or MOPS buffer and adjusted to respective pH using NaOH or HCl, whereas 200 mM stock solutions of the coacervation peptides were prepared in water with 500 mM NaOH added. The 80 mM Tyr stock solution was prepared in 500 mM sodium carbonate buffer at pH = 10.5.

The 2 M stock solution of pyridine, the stock solutions of the polycations (500 mM R10, R30), and the 10% PEG8000 stock solution were prepared in MQ-water and stored at 8 °C. Reaction cycles were started by the addition of the high concentration (2 M or 250 mM) MAP to the solution. All experiments were carried out at room temperature or 25 (±0.5).

Kinetic model. A kinetic model written with COPASI 4.36 (Build 260) was used to predict the evolution of the reaction network over time. The constants were fitted to the ^{31}P-NMR kinetic measurements, and the concentrations of compounds were calculated every five minutes. The rate constants are given in Table S7.

Elemental analysis. The CHNS values are determined simultaneously by combustion analysis in a EuroEA Elemental Analyser from HEKAtech. The following standard substances were included in the analyses: 2x BBOT and 1x chloro-2,4-dinitrobenzene. An error tolerance range of ± 0.3% can be specified. Potassium was determined using acid digestion and subsequent measurement on an Agilent 280 FS-AA atomic absorption spectrometer (flame AAS). Potassium dihydrogen phosphate was used as the reference substance. The error tolerance range is +- 0.5%. Phosphorus was determined after acid digestion and subsequent measurement on a Cary100 UV/VIS photometer from Agilent. Triphenylphosphine was used as the test substance. The error tolerance range is +- 0.3%. As obtained from the central analytics of the Technical University of Munich.

^{1}H Nuclear magnetic resonance spectroscopy (NMR). ^{1}H-NMR spectra were recorded on a Bruker AV-500HD NMR spectrometer. All chemical shifts δ are given in parts per million (ppm) and referenced to the residual proton signal of dimethylsulfoxide-d_6 (δ = 2.50 ppm). The NMR spectra were analyzed using MestReNova© software (version 14.2.3-29241).

^{31}P-NMR spectroscopy kinetic measurements. Over time, the fuel consumption, formation, and hydrolysis of phosphorylated compounds were monitored with ^{31}P-NMR on a Bruker AV500CR NMR-spectrometer. An inverse gated H-decoupled[3] method with 16 scans and 25 s relaxation delay was used. As internal standard, phosphonoacetic acid (20 mM, δ = 15.7 ppm[4]) was used. The concentrations were calculated by using the following equation[3]:

$$c_x = c_{standard} \times \frac{integral_x}{integral_{standard}} \quad \text{(eq. 1)}$$

With c_x: concentration of compound x, $c_{standard}$: concentration of the internal standard, $integral_x$: integral of compound x, $integral_{standard}$: integral of internal standard.

For ^{31}P-NMR kinetic measurements, 200 µL (Ac-GHG-OH) or 500 µL (amino acids, hydrolysis) of the samples were prepared. The samples consisted of 500 mM MES or MOPS buffered solution of 75 mM amino acid (sodium carbonate for 60 mM Tyr) or Ac-GHG-OH in the presence and absence of pyridine, and the addition of 80 mM MAP started the reaction. The hydrolysis of MAP at different pH and fuel consumption, respectively, and the formation of the transient species were determined by applying eq. 2. The NMR spectra were analyzed using MestReNova© software (version 14.2.3-29241).

To determine the reaction rate constants k_{py} at different pH values, samples consisted of 500 mM MES or MOPS buffered solution of 80 mM MAP in the presence of 15 mM pyridine (pH 5.5 and 6.5) and 5 mM (pH 7.5).

pH measurements. A pH meter (HANNA HI 2211 pH/ORP Meter) with an Ag/AgCl electrode was used for the pH adjustments of the stock solutions and pH value measurements. It was calibrated with standard calibration solutions (pH = 7.01 and 4.01) each time before usage.

ESI-MS. An LCQ Fleet Ion Trap Mass Spectrometer (Thermo Scientific) was used for ESI-MS experiments. The data was evaluated using the Thermo Xcalibur Qual Browser 2.2 SP1.48 software. The fractions of the preparative HPLC were collected, and 2 µL was injected directly into the loop.

ITC measurements. ITC experiments were performed with a MicroCal PEAQ-ITC from Malvern Pananalytical. All experiments were performed at 25 °C. The following conditions were used: R30 (15 mM charges, 500 µM strand in MOPS 100 mM, pH 7.5) was titrated with the Ac-Y(OMe)DHDD-OH (10 mM in 100 mM MOPS, pH 7.5): 26 injections, 3 µL each. A control was performed by titrating the corresponding amount of peptide in 100 mM MOPS

buffer (pH 7.5) and used to correct for dilution enthalpy. Data were fitted to a single set of sites binding isotherm using the PEAQ-ITC Analysis software.

Analytical HPLC kinetic measurements. For the kinetic measurement of the transient 1- and 3-phospho isomers of the Ac-Y(OMe)DHDD-NH_2, an analytical HPLC (Vanquish SINGLE HPLC system with EC 150/4 NUCLEODUR C_{18} Pyrmid, 3 µm (particle size: 3 µm, length: 150 mm, ID: 4 mm), Machery-Nagel; eluted with a gradient of TEAA 25 mM and ACN:TEAA 25 mM 25:75 at 30 °C) was used. The Chromeleon 7 Data System Software (Version 7.3.1) was used to evaluate the received data.

For the experiments, samples consisted of 20 mM Ac-Y(OME)DHDD-NH_2 and 12.5/25 mM MAP in a 100 mM MOPS buffered solution. The reaction was started by adding MAP, and the reaction solution was transferred to inserts for a 1.5 mL screw cap HPLC glass vial. 1 µL of the solution was injected without any further dilution. A linear gradient of TEAA 25 mM and ACN:TEAA 25 mM 25:75 at 30 °C column temperature (TEAA = triethylammonium acetate pH = 7) composed as described below was used.

Calibration curves for the peptide (in MQ water) were performed in triplicate with the corresponding method. Retention times and calibration values are given in Supporting Table S3.

UV/Vis Spectroscopy. The UV/Vis measurements were carried out using a Multiskan FC (ThermoFisher) microplate reader. Samples (50 µL) were prepared in Eppendorf tubes and transferred into a 96 half-area well-plate (tissue culture plate, non-treated). The temperature (25 (±0.5ºC) was set 10 min before starting the measurement. Each experiment was performed at 500 nm, and every 5 min, a data point was acquired. (N = 3)

For absorbance/optical density experiments, 50 µL sample volumes were prepared. The samples consisted of 20 mM Ac-Y(OME)DHDD-NH_2, 50 mM R30 (in positive charges), 0, 5, 7.5, 10, 12.5, 15, 20, 25, 37.5, 50 mM MAP (+x mM Pi) in a 100(-x) mM MOPS pH 7.5 buffered solution. To sustain the ionic strength of the system for samples fuelled with less than 12.5 mM MAP, the missing amount of P_i was added, and for samples fuelled with more than 12.5 mM MAP, the buffer concentration was reduced (buffer and Na+ were considered).

Confocal Fluorescence Microscopy. A Leica SP5 confocal microscope using a 63x oil immersion objective was used to image the droplets in microreactors. Coacervates were dyed with the fluorophore Sulforhodamine B and Cy5-R30, which were excited at 561 nm and 638 nm and detected from 566-642 nm and 643-839 nm with a HyD detector. The pinhole was set to 1 Airy unit. Micrographs of the microfluidic droplets were acquired in z-stacks with 1 µm between z-planes to analyze the evolution of coacervates in the entire microfluidic droplets.

The micrographs were recorded with a resolution of 1024 x 1024 pixels or 512 x 512 pixels at 1x zoom and 600x scan speed (bidirectional scan). Measurements were performed at 21 °C, but the samples were incubated at 25 °C. ImageJ (Version 2.14.0) was used to analyze the micrographs.

For confocal experiments, 25 µL (snipping method) or 150 µL (microfluidic setup) sample volume was prepared. If not mentioned differently, the samples consisted of 20 mM Ac-Y(OMe)DHDD-NH_2 (15 mM Ac-Y(OMe)DHDD-OH, 50 mM R30 (positive charges), 200 nM SR, 500 nM Cy5-R30 and 12.5 mM MAP/P_i in a 100 mM MOPS buffered solution. First, MOPS, peptide, and dyes were combined, and the reaction started with adding MAP. After the agitation of the reaction, solution R30 was added, and it was proceeded with the water in oil emulsion preparation.

For the partition experiments of the non-functional structures instead of dyes, 200 nM of the Cy3-labelled structures were added and the samples were prepared with the snipping method.

Sequences of the non-functional structures.

ssDNA	$(AGTC)_8$
daDNA	$(ATCG)_8$
RNA	U_{30}
pSS	109 monomer units, 22.5 kDa

Microfluidic chip preparation. Microfluidic PDMS (Polydimethylsiloxane, Sylgard 184, Dow Corning)-based devices were designed with QCAD-pro (RibbonSoft GmbH) and fabricated using photo- and soft-lithography[5] as previously described[6-7].

Water in oil emulsion preparation. The water in oil emulsions was prepared either with a microfluidic droplet generator or with a snipping technique. HFE oil with 1.33% fluoro-surfactant was used for both types of sample preparation. A pump setup for microfluidics and a microfluidic chip were used to obtain standardized water droplet sizes. The chip has two inlets for the oil and the reaction mixture. A pressure of 610 mbar was applied to both channels, and the emulsion was collected from the outlet. For the snipping method, 5 µL of the reaction solution was added to 50 µL of the HFE oil with 1.33% fluoro-surfactant and snipped against the tube. Both emulsions were pipetted below a glass slide, glued onto another glass slide with double-sided sticky tape, and sealed with two-component glue.

Fluorescence recovery after photobleaching. A Leica SP8 confocal microscope with a 63x water immersion objective was used to perform FRAP experiments. The samples were prepared as described previously described. Cy5-R30 was bleached with a 638 nm laser and imaged at 648-784 nm with a PMT. The pinhole was set to 1 Airy unit, and the images were acquired at a resolution of 254 x 254 pixels. Recovery data was background and photofading corrected by using the following equation. [8]

$$I_{corrected}(t) = \frac{I_{raw}(t) - I_{background}(t)}{I_{fading}(t) - I_{background}(t)} \quad \text{(eq. 2)}$$

With $I_{corrected}(t)$: background and photofading corrected fluorescence intensity at time point t, $I_{raw}(t)$: raw fluorescence intensity at time point t, $I_{background}$: fluorescence intensity of background at time t, and $I_{fading}(t)$: fluorescence intensity of a neighboring not bleached droplet at time point t.

The corrected intensities were normalized by the prebleach intensity:[8]

$$I_{normalized}(t) = \frac{I_{corrected}(t)}{I_{prebleach}} \quad \text{(eq. 3)}$$

With $I_{normalized}(t)$: normalized fluorescence intensity, $I_{prebleach}$: fluorescence intensity before bleaching.

For the fit of the FRAP recovery time trace, the following equation was used:[9]

$$I_{normalized}(t) = \frac{a + b(\frac{t}{\tau_{1/2}})}{1 + \frac{t}{\tau_{1/2}}} \quad \text{(eq. 4)}$$

With a, b, and $\tau_{1/2}$: fitting parameters. $\tau_{1/2}$: recovery half-time.

The diffusivity constant was calculated using following equation:[9]

$$D = \backslash \frac{r^2}{\tau_{1/2}} \quad \text{(eq. 5)}$$

With D: diffusivity constant and r: radius of the bleach spot (r was determined by the region of interest used as $I_{raw}(t)$).

Supporting Notes. Description of the kinetic model and reaction rate constants.

A kinetic model was written in COPASI that described each reaction involved in the chemical reaction network. The concentrations of each reactant were calculated for every 5 minutes in the cycle. The model was used to obtain fitted curves based on ^{31}P-NMR or HPLC data that described the evolution of the concentration of the phosphorylated species, fuel, and waste. The fitted reaction rate constant values of the hydrolysis in the presence of pyridine and of the phosphorylation of H were combined and used while fitting the k-values for the phosphorylation in the presence of pyridine.

The *Levenberg-Marquardt* method was used to obtain the k-values, and the deterministic (LSODA) method was used to obtain the time courses.

Reaction 0 (k_0)

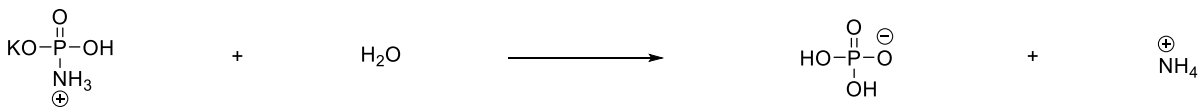

Scheme S1 | Kinetic model – Reaction 0 (k_0): direct hydrolysis of MAP.

The direct hydrolysis of the fuel (MAP) to inorganic phosphate follows pseudo-first-order kinetics with respect to MAP. The rate constants and the corresponding half-lives are summarized in Table S7.

Reaction 1 (k_1)

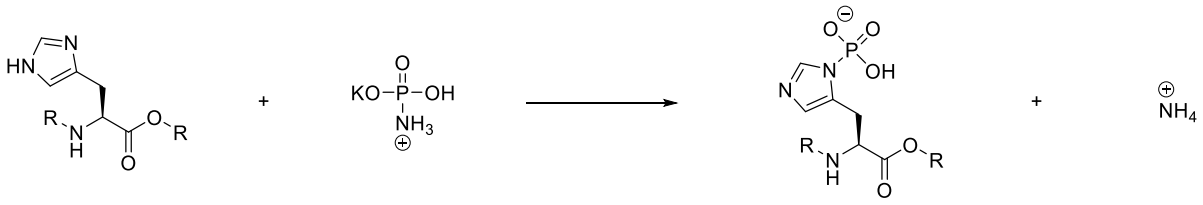

Scheme S2 | Kinetic model – Reaction 1 (k_1): Formation of 1-pH.

The reaction of MAP with the H-precursor to the 1-pH-product follows second-order kinetics. The rate constants are shown in Table S7.

Reaction -1 (k_{-1})

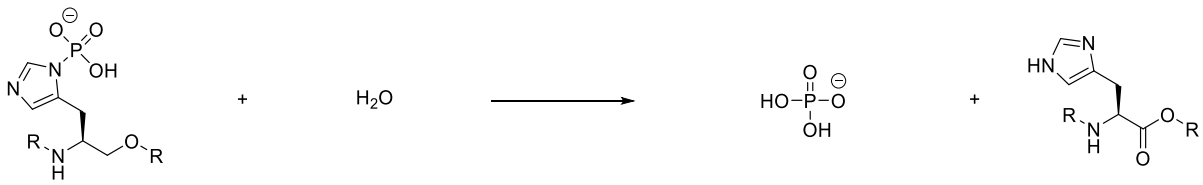

Scheme S3 | Kinetic model – Reaction -1 (k_{-1}): Hydrolysis of 1-pH.

The hydrolysis of 1-pH follows pseudo-first-order kinetics with respect to 1-pH. The rate constants are shown in Table S7.

Reaction 2 (k_2)

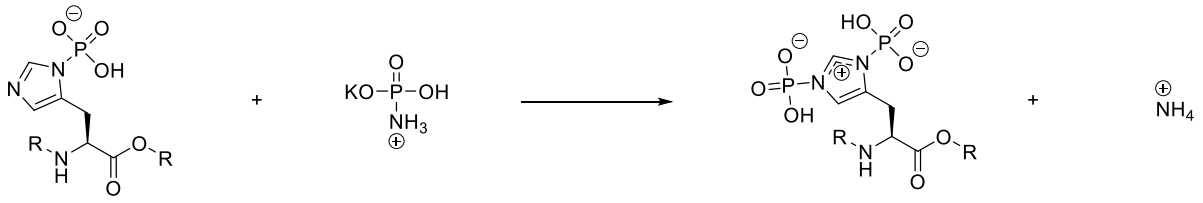

Scheme ~~S~~4 | Kinetic model – Reaction 2 (k_2): Formation of 1,3-bpH.

The reaction of MAP with 1-pH to the 1,3-bpH-product follows second-order kinetics. The bisphosphorylated species was only observed for histidine and Ac-GHG-OH at pH = 7.5. The rate constants are shown in Table S7.

Reaction -2 (k_{-2})

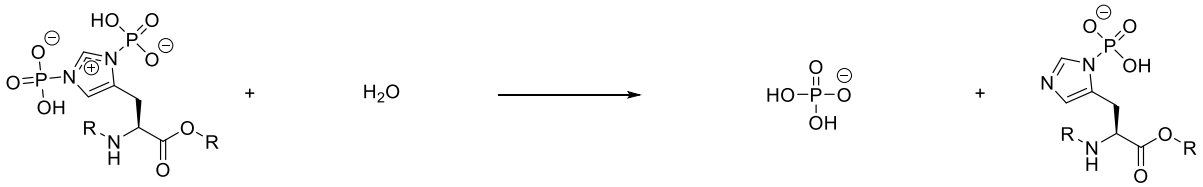

Scheme S5 | Kinetic model – Reaction -2 (k_{-2}): Hydrolysis of 1,3-bpH.

The hydrolysis of 1,3-bispH to 1-pH follows pseudo-first-order kinetics with respect to the 1-phospho-group of 1,3-bispH. The rate constants are shown in Table S7.

Reaction 3 (k_3)

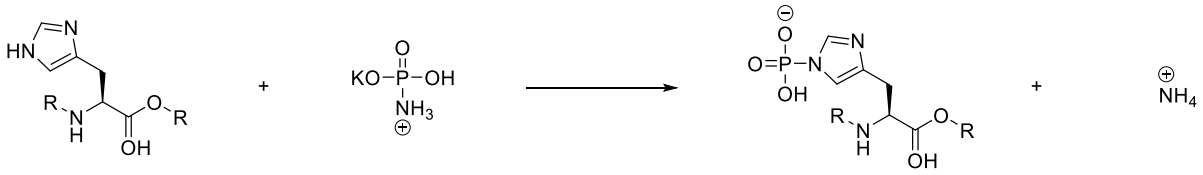

Scheme S6 | Kinetic model – Reaction 3 (k_3): Formation of 3-pH.

The reaction of MAP with the H-precursor to the 3-pH-product follows second-order kinetics. The rate constants are shown in Table S7.

Reaction -3 (k_{-3})

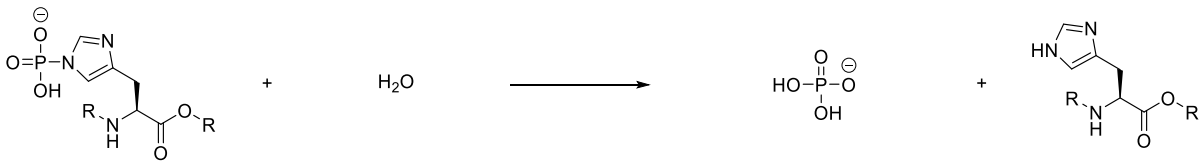

Scheme S7 | Kinetic model – Reaction -3 (k_{-3}): Hydrolysis of 3-pH.

The hydrolysis of 3-pH follows pseudo-first-order kinetics with respect to 3-pH. The rate constants for H and Ac-GHG-OH were determined experimentally *via* ^{31}P-NMR by monitoring the concentration profiles after the fuel was consumed. The rate constants are shown in Table S7. To compare the evolution of Ac-G(3-pH)G-OH in the presence of pyridine, the apparent first-order constant k'_{-3p} was introduced. After the fuel was consumed, it was assumed that the hydrolysis follows pseudo-first-order kinetics. The apparent rate constants in the presence of pyridine are summarized in Table S8.

Reaction 4 (k_4)

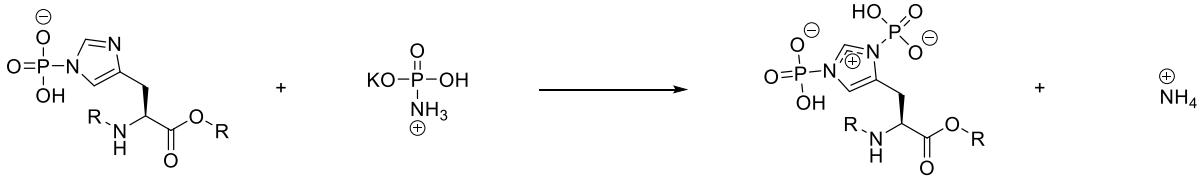

Scheme S8 | Kinetic model – Reaction 4 (k_4): Formation of 1,3-bpH.

The reaction of MAP with 3-pH to the 1,3-bpH-product follows second-order kinetics. The bisphosphorylated species was only observed for H and Ac-GHG-OH at pH = 7.5. The rate constants are shown in Table S7.

Reaction -4 (k_{-4})

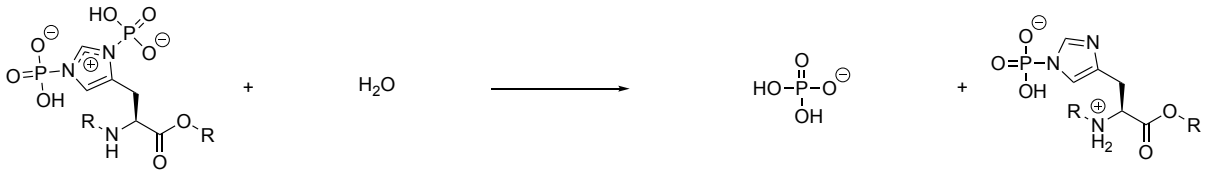

Scheme S9 | Kinetic model – Reaction -4 (k_{-4}): Hydrolysis of 1,3-bpH.

The hydrolysis of 1,3-bpH to 3-pH follows pseudo-first-order kinetics with respect to the 3-phospho-group of 1,3-bpH. The rate constants are shown in Table S7.

Reaction py (k_{py})

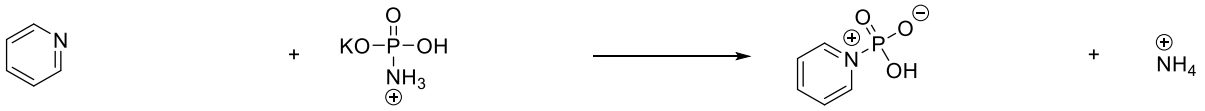

Scheme S10 | Kinetic model – Reaction py (k_{py}): Formation of pyridinio-N-phosphonate.

The reaction of MAP with pyridine to pyridinio-*N*-phosphonate follows second-order reaction kinetics. k_{py} values were fitted with COPASI to experimental data. The rate constants are shown in Table S7.

Reaction -py (k_{-py})

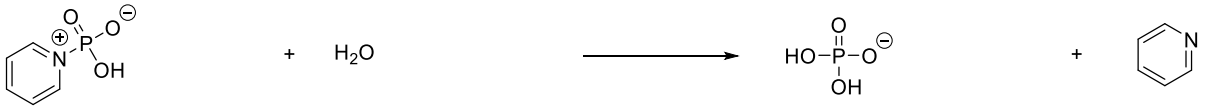

Scheme S11 | Kinetic model – Reaction -py (k_{-py}): Hydrolysis of pyridinio-N-phosphonate.

The hydrolysis of pPy to pyridine and phosphate follows pseudo-first-order kinetics with respect to pPy. k_{-py} values were fitted with COPASI to experimental data. The rate constants are shown in Table S7.

Reaction 5 (k_5)

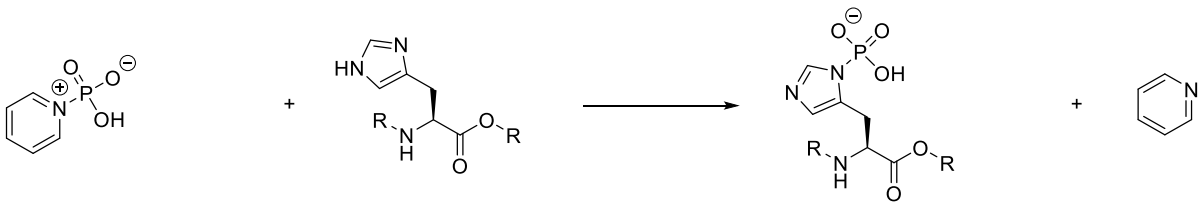

Scheme S12 | Kinetic model – Reaction 5 (k_5): Formation of 1-pH.

The reaction of pPy with H to the 1-pH-product follows second-order kinetics. The rate constants are shown in Table S7.

Reaction -5 (k_{-5})

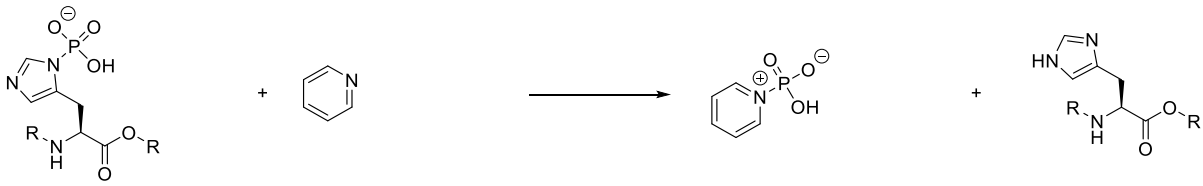

Scheme S13 | Kinetic model – Reaction -5 (k_{-5}): Dephosphorylation of 1-pHis with pyridine.

The reaction of 1-pH with pyridine to form pPy and His follows second-order kinetics. The rate constants are shown in Table S7.

Reaction 6 (k_6)

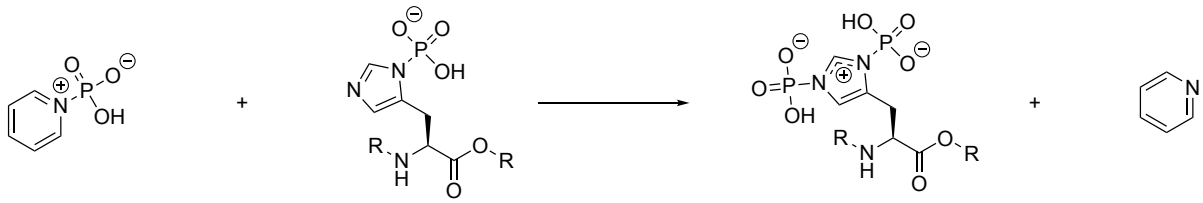

Scheme S14 | Kinetic model – Reaction 6 (k_6): Formation of 1,3-bpH.

The reaction of pPy with 1-pH to the 1,3-bpH-product follows second-order kinetics. The rate constants are shown in Table S7.

Reaction -6 (k_{-6})

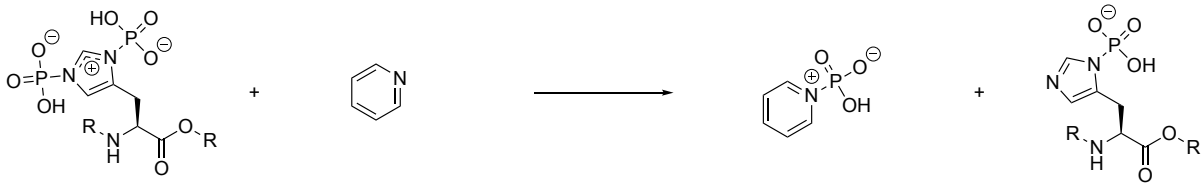

Scheme S15 | Kinetic model – Reaction -6 (k_{-6}): Dephosphorylation of 1,3-bpH with pyridine.

The reaction of 1,3-bpH with pyridine to form pPy and 1-pH follows second-order kinetics. The rate constants are shown in Table S7.

Reaction 7 (k_7)

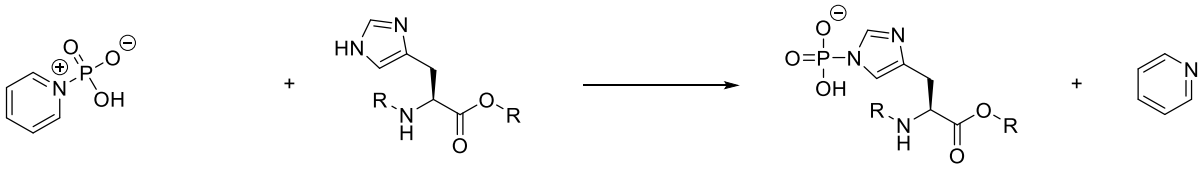

Scheme S16 | Kinetic model – Reaction 7 (k_7): Formation of 3-pH.

The reaction of pPy with His to the 3-pH-product follows second-order kinetics. The rate constants are shown in Table S7.

Reaction -7 (k_{-7})

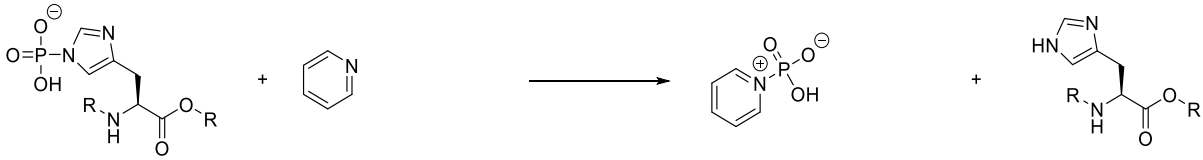

Scheme S17 | Kinetic model – Reaction -7 (k_{-7}): Dephosphorylation of 3-pH with pyridine.

The reaction of 3-pH with pyridine to form pPy and His follows second-order kinetics. The rate constants are shown in Table S7. To compare the evolution of Ac-G(3-pH)G-OH in the presence of pyridine, the apparent first-order constant k'_{-3} was introduced. After the fuel was consumed, it was assumed that the hydrolysis follows pseudo-first-order kinetics. The apparent rate constants in the presence of pyridine are summarized in Table S8.

Reaction 8 (k_8)

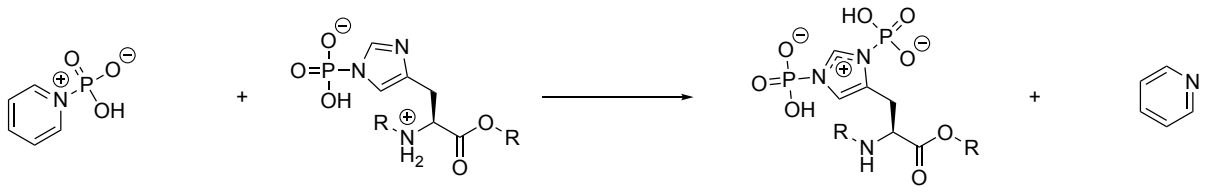

Scheme S18 | Kinetic model – Reaction 8 (k_8): Formation of 1,3-bpH.

The reaction of pPy with 3-pH to the 1,3-bpH-product follows second-order kinetics. The rate constants are shown in Table S7.

Reaction -8 (k_{-8})

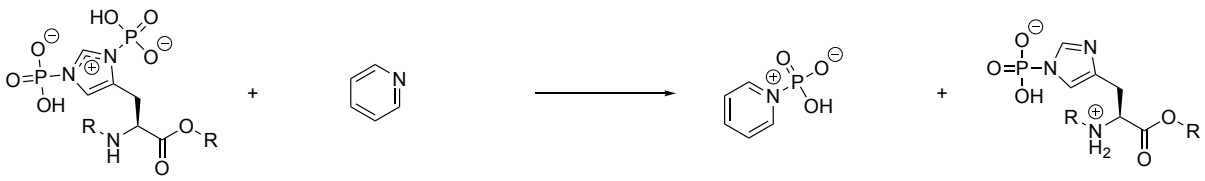

Scheme S19 | Kinetic model – Reaction -8 (k_{-8}): Dephosphorylation of 1,3-bpH with pyridine.

The reaction of 1,3-bpH with pyridine to form pPy and 3-pH follows second-order kinetics. The rate constants are shown in Table S7.

$$\frac{d[MAP]}{dt} = -k_0[MAP] - k_1[MAP][H] - k_2[MAP][1-pH] - k_3[MAP][H] - k_4[MAP][3-pH] - k_{Py}[MAP][Py]$$

$$\frac{d[Pi]}{dt} = +k_0[MAP] + k_{-1}[1-pH] + k_{-2}[1,3-bpH] + k_{-3}[3-pH] + k_{-4}[1,3-bpH] + k_{-Py}[pPy]$$

$$\frac{d[H]}{dt} = +k_1[MAP][H] + k_{-1}[1-pH] - k_3[MAP][H] + k_{-3}[3-pH] - k_5[pPy][H] + k_{-5}[Py][1-pH] - k_7[pPy][H] + k_{-7}[Py][3-pH]$$

$$\frac{d[1-pH]}{dt} = +k_1[MAP][H] - k_{-1}[1-pH] - k_2[MAP][1-pH] + k_{-2}[1,3-bpH] + k_5[pPy][H] - k_{-5}[Py][1-pH] - k_6[pPy][1-pH] + k_{-6}[Py][1,3-bpH]$$

$$\frac{d[3-pH]}{dt} = +k_3[MAP][H] - k_{-3}[3-pH] - k_4[MAP][1-pH] + k_{-4}[1,3-bpH] + k_7[pPy][H] - k_{-7}[Py][3-pH] - k_8[pPy][3-pH] + k_{-8}[Py][1,3-bpH]$$

$$\frac{d[1,3-bpH]}{dt} = +k_2[MAP][1-pH] - k_{-2}[1,3-bpH] + k_4[MAP][3-pH] - k_{-4}[1,3-bpH] + k_6[pPy][1-pH] - k_{-6}[Py][1,3-bpH] + k_8[pPy][3-pH] - k_{-8}[Py][1,3-bpH]$$

$$\frac{d[Py]}{dt} = -k_{Py}[MAP][Py] + k_{-Py}[pPy] + k_5[pPy][H] - k_{-5}[Py][1-pH] + k_7[pPy][H] - k_{-7}[Py][3-pH] + k_6[pPy][1-pH] - k_{-6}[Py][1,3-bpH] + k_8[pPy][3-pH] - k_{-8}[Py][1,3-bpH]$$

$$\frac{d[Ppy]}{dt} = +k_{Py}[MAP][Py] - k_{-Py}[pPy] - k_5[pPy][H] + k_{-5}[Py][1-pH] - k_7[pPy][H] + k_{-7}[Py][3-pH] - k_6[pPy][1-pH] + k_{-6}[Py][1,3-bpH] - k_8[pPy][3-pH] + k_{-8}[Py][1,3-bpH]$$

Scheme S20 | System of differential equations used.

Table S1 | Rate constants used in the kinetic model for the cycle with Ac-GHG-OH in the presence of pyridine.

	pH 5.5 (Ac-GHG-OH)	**pH 6.5 (His)**	**pH 6.5 (Ac-GHG-OH)**	**pH 7.5 (Ac-GHG-OH)**	**pH 7.5 (acY'DHDDam)**
k_0 [h^{-1}]	6.22 ± 0.46e-2 [a]	4.20 ± 0.06 e-2 [a]	4.20 ± 0.06 e-2 [a]	3.34 ± 0.17e-2 [a]	3.34 ± 0.17e-2 [a]
k_1 [$L^*(mmol^*h)^{-1}$]	1.00 ± 1.65e-5	1.14 ± 0.11 e-3	1.45e-4 ± 9.97e-6	2.47 ± 0.10 e-4	1.37 ± 0.21 e-3
k_{-1} [h^{-1}]	2.24e1 ± 2.52e3	1.79 ± 0.14	3.89 ± 0.27 e-1	2.10 ± 0.10 e-1	1.40 ± 0.18
k_2 [$L^*(mmol^*h)^{-1}$]	n/a	1.58e-05 ± 9.56e-4	n/a	2.01 ± 0.24 e-3	0
k_{-2} [h^{-1}]	n/a	2.40 ± 1.17 e-1	n/a	3.61 ± 0.71 e-2	0
k_3 [$L^*(mmol^*h)^{-1}$]	4.70e-5 ± 9.56e-07	8.68 ± 0.96e-4	1.79e-4 ± 5.69 e-06	4.89e-4 ± 0.19e-5	3.30 ± 0.37e-4
k_{-3} [h^{-1}]	1.40 ± 0.16e-2[a]	6.56 ± 0.43e-2[a]	1.16 ± 0.13e-2[a]	4.93 ± 0.58e-3[a]	6.71 ± 2.01 e-3
k_4 [$L^*(mmol^*h)^{-1}$]	n/a	2.35 ± 0.65e-3	n/a	6.96e-6 ± 6.07e-5	0
k_{-4} [h^{-1}]	n/a	3.69 ± 0.2e-1	n/a	1e-06 ± 9.01e-3	0
k_{py} [$L^*(mmol^*h)^{-1}$]	8.37 ± 1.12e-3	n/a	1.55 ± 0.39 e-2	1.70 ± 0.09 e-2	n/a
k_{-py} [h^{-1}]	1e+6 ± 1.32e+11	n/a	1e+6 ± 2.45e+11	4.90e+6 ± 4.12e+10	n/a
k_5 [$L^*(mmol^*h)^{-1}$]	1e-6 ± 5.72e-4	n/a	811 ± 59.0	8.52e+3 ± 4.22e+2	n/a
k_{-5} [$L^*(mmol^*h)^{-1}$]	8.57e-2 ± 2.13e+3	n/a	1e-6 ±7.69e-4	3.54 ± 0.58e-3	n/a
k_6 [$L^*(mmol^*h)^{-1}$]		n/a	2.23e+3 ± 1.12e+2	4.45e+4 ± 3.03e+3	n/a

k_{-6} [L*(mmol*h)$^{-1}$]		n/a	2.11 ± 0.14e-3	1e-6 ± 1.18e-5	n/a
k_7 [L*(mmol*h)$^{-1}$]	382 ± 2.75e+3	n/a	n/a	1.90 ± 0.89 e+4	n/a
k_{-7} [L*(mmol*h)$^{-1}$]	2.17 ± 0.50e-3	n/a	n/a	1.40e-3 ± 7.58e-5	n/a
k_8 [L*(mmol*h)$^{-1}$]	n/a	n/a	n/a	3.35e-6 ± 3.47e-2	n/a
k_{-8} [L*(mmol*h)$^{-1}$]	n/a	n/a	n/a	4.50 ± 0.23e-3	n/a

[a] experimentally determined

Table S2 | Apparent hydrolysis of MAP in with 75 mM different amino acids in a 500 mM MOPS buffered solution.

Amino acid	Apparent hydrolysis constant of MAP k'_0 [h^{-1}]
His	2.34 ± 0.11e-1
Arg	4.71 ± 0.05e-2
Lys	4.70 ± 0.02e-2
Cys	4.80 ± 0.07e-2
Ser	4.80 ± 0.07e-2
Tyr[a]	9.00 ± 4.67e-4
Asp	4.88 ± 0.14e-2

[a]sodium carbonate buffer at pH 10.5.

Table S3 | Apparent first-order constants for hydrolysis k'_{-3pH} ([h^{-1}]) of 3-pH in the presence of pyridine.

Concentration of pyridine [mM]	**5.5**	**6.5**	**7.5**
5	4.50 ± 0.80e-2	1.83 ± 0.10e-2	9.03 ± 1.62e-3
15		3.55 ± 0.86e-2	2.45 ± 0.02e-2
25		6.13 ± 1.23e-2	4.36 ± 0.69e-2

Supporting Figures

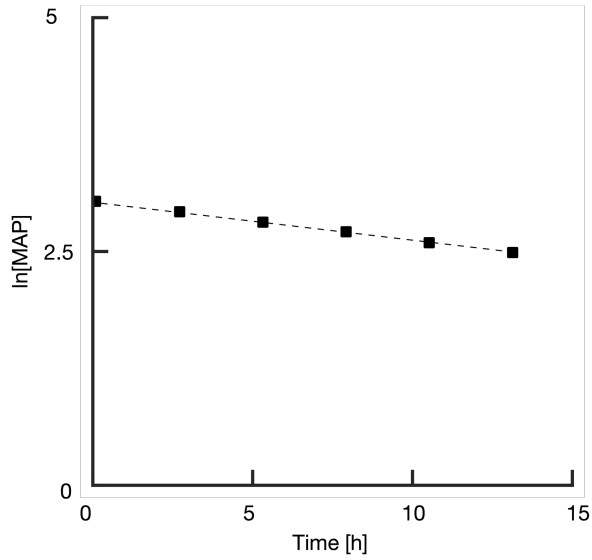

Figure S1 | Representative empirical determination of the pseudo-first-order hydrolysis of 20 mM MAP in a 500 mM MES buffered solution at pH 6.5. (The error bars represent the standard deviation from the mean with n = 3).

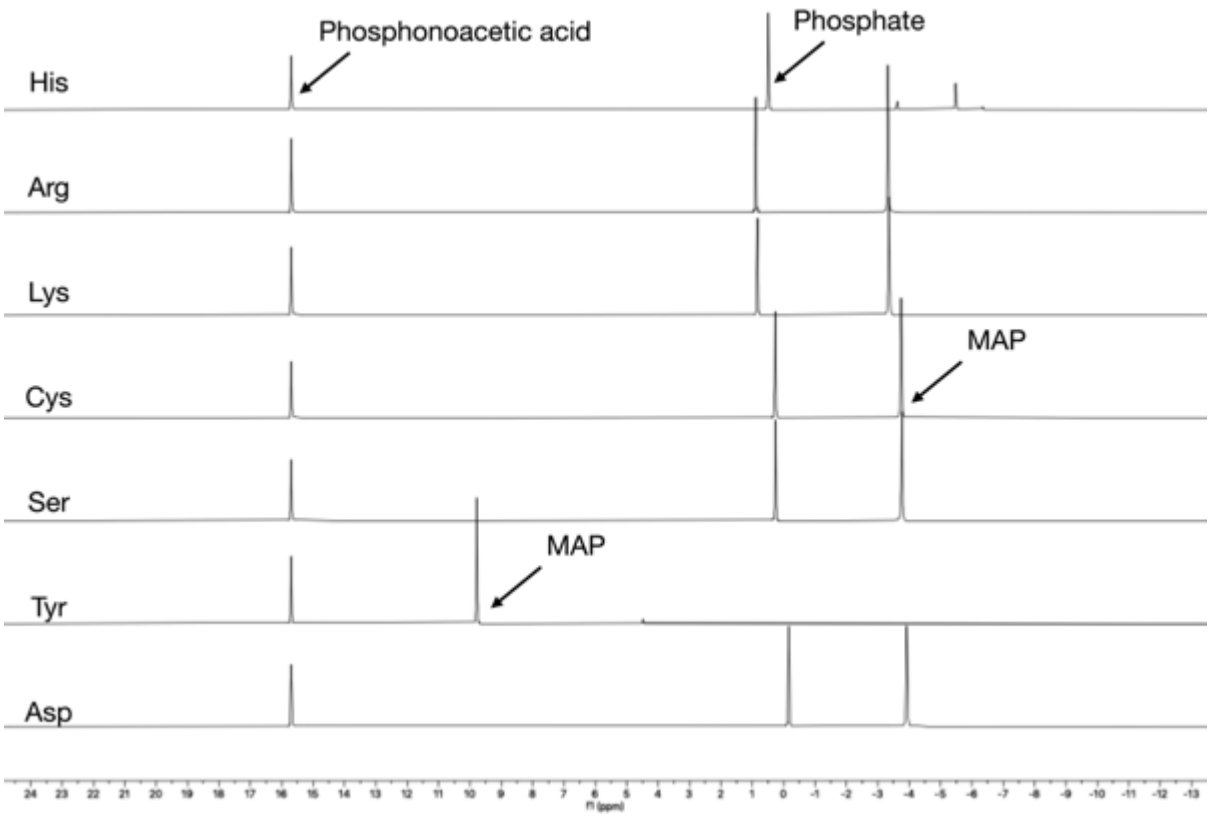

Figure S2 | Representative ^{31}P-NMR spectra of the consumption of MAP in the presence of different amino acids after 60 h (75 mM amino acid and 80 mM MAP in 500 mM MES buffered solution pH 6.5. 60 mM Tyr and 80 mM MAP in 500 mM sodium carbonate solution pH 10.5).

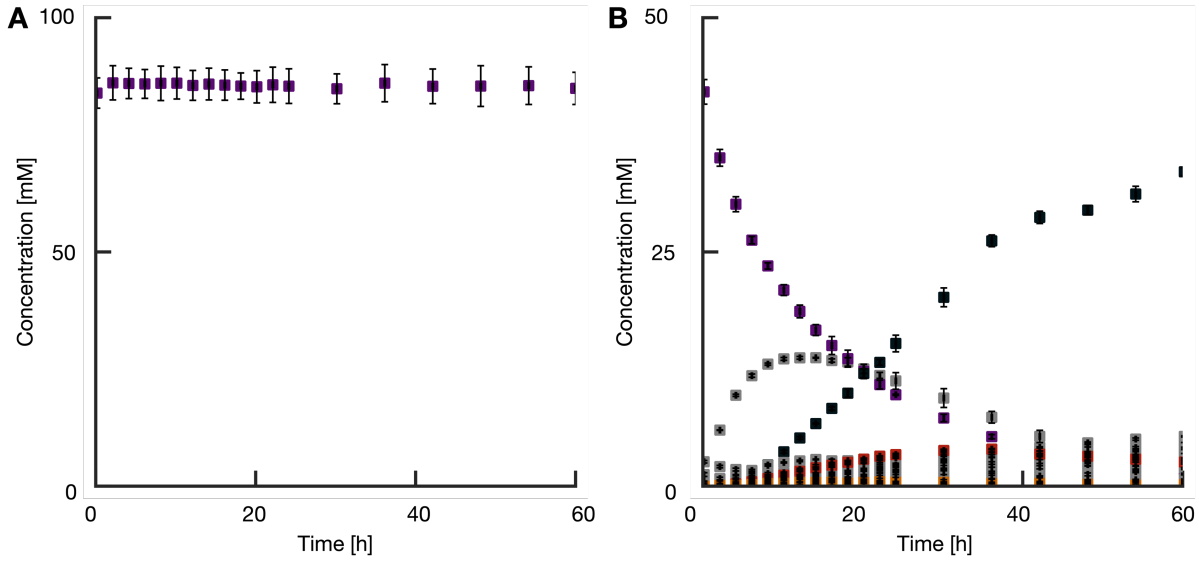

Figure S3 | Investigation of different biologically relevant fuels (purple) **A.** trimetaphosphate (TMP) and **B.** diamidophosphate (DAP). Concentration profiles of the phosphorous-containing compounds were recorded with ^{31}P-NMR. **A.** Phosphorylation of H in the presence of TMP (purple). No conversion. **B.** Phosphorylation of H in the presence of DAP (purple). 1-pH is highlighted in yellow, 3-pH in red. (The error bars represent the standard deviation from the mean with n = 3).

The hydrolysis constant of DAP in a 500 mM MES buffered solution at pH = 6.5 is k_0 = 3.97 ± 0.91e-3 h^{-1}, whereas the apparent hydrolysis constant in the presence of 75 mM H k'_0 = 5.65 ± 0,13e-2 h^{-1} is increased.

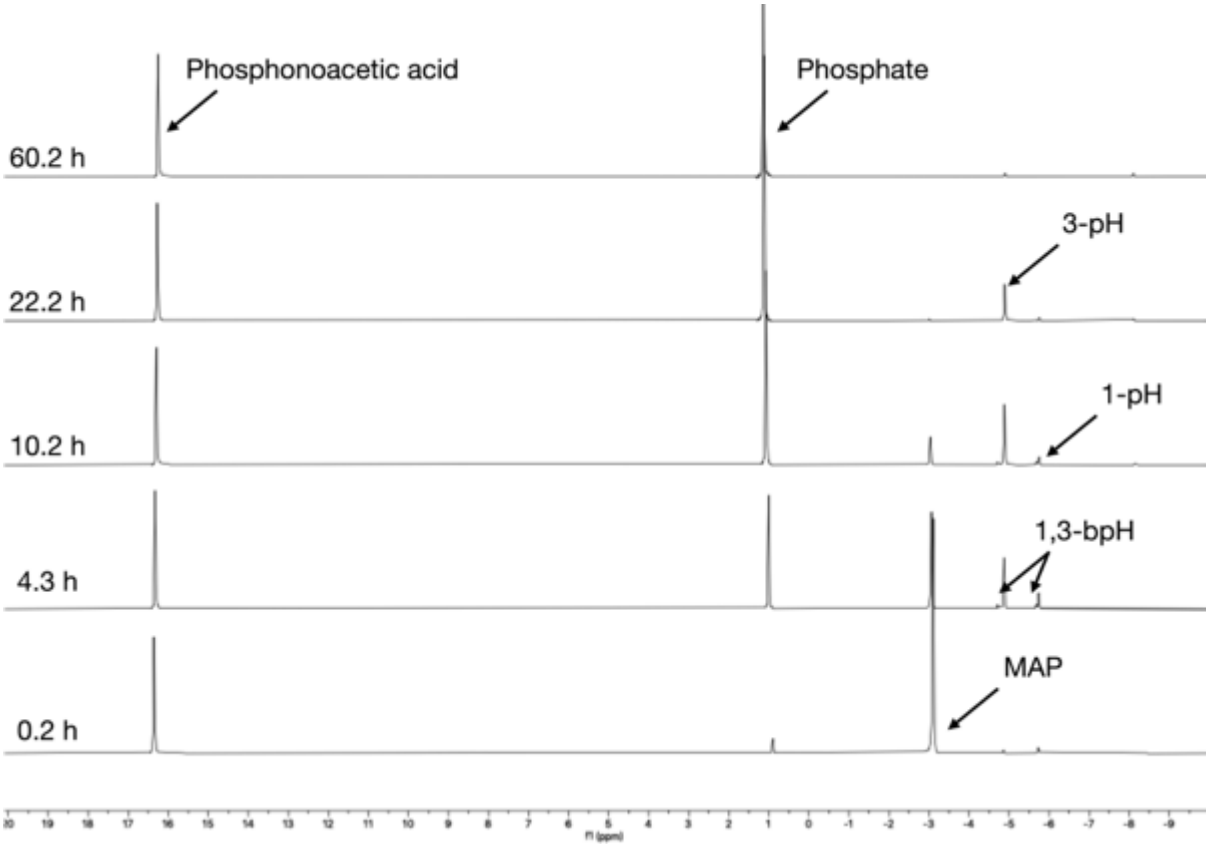

Figure S4 | Representative time evolution of the chemical shifts in the ^{31}P-NMR spectra of the phosphorylation of H at the expense of MAP (75 mM H and 80 mM MAP in 500 mM MES buffered solution pH 6.5).

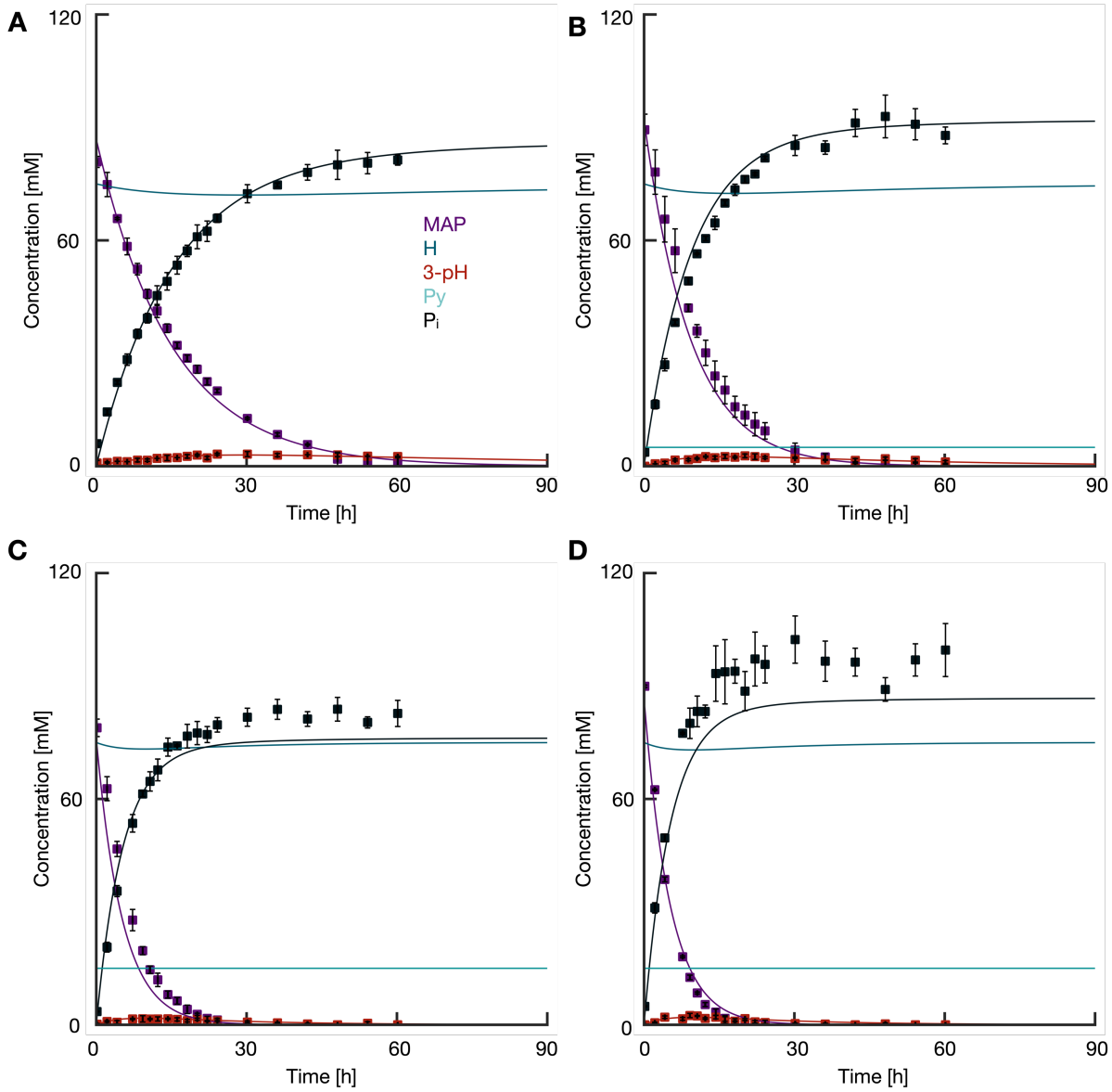

Figure S5 | Concentration profiles (squares) and kinetic profiles (lines) of the phosphorylation cycle of Ac-GHG-OH with MAP at pH 5.5 and following pyridine concentrations **A.** 0, **B.** 5, **C.**15, and **D.** 25 mM recorded with ^{31}P-NMR. (The error bars represent the standard deviation from the mean with n = 3).

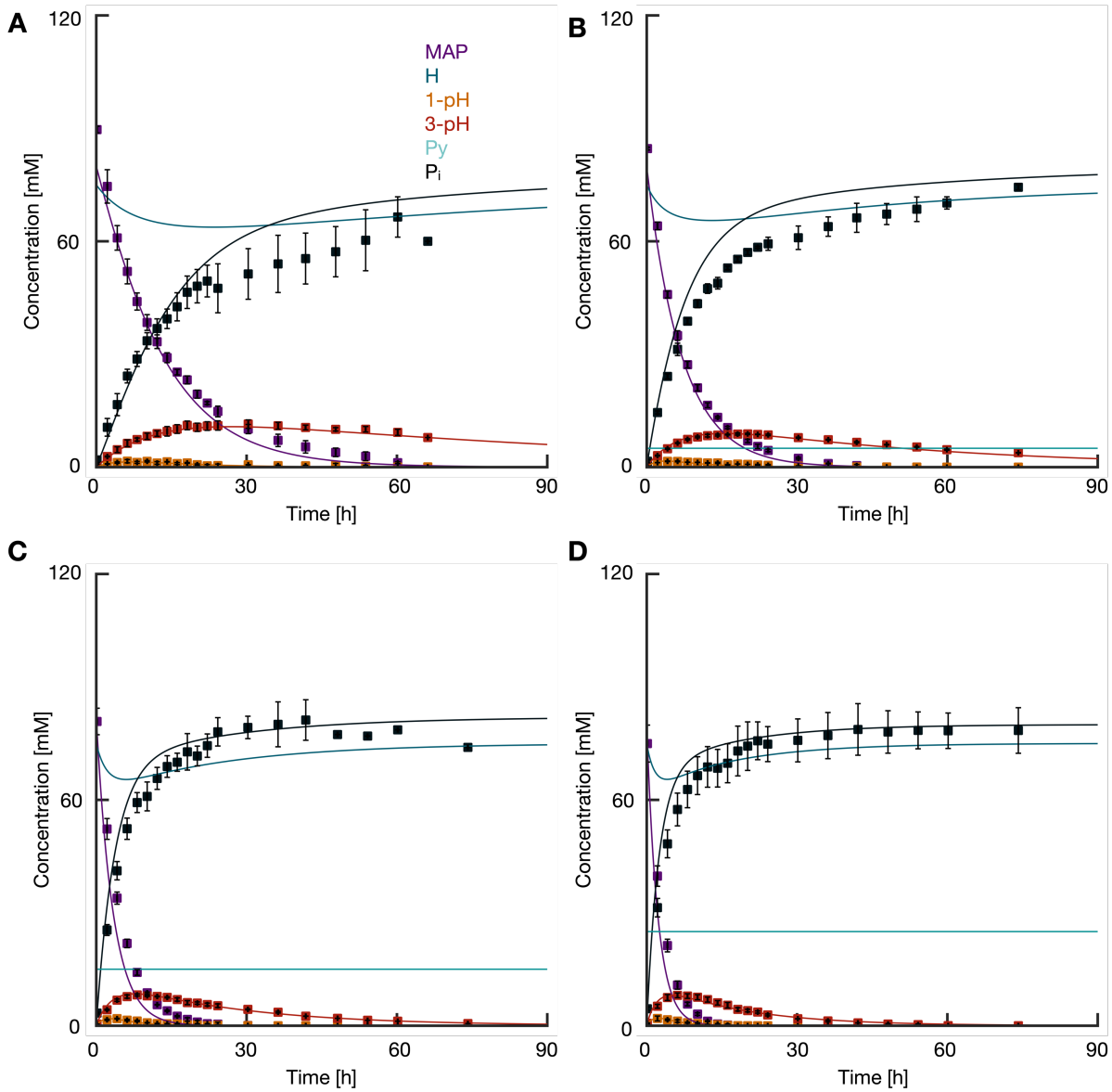

Figure S6 | | Concentration profiles (squares) and kinetic profiles (lines) of the phosphorylation cycle of Ac-GHG-OH with MAP at pH 6.5 and following pyridine concentrations **A.** 0, **B.** 5, **C.**15, and **D.** 25 mM recorded with ^{31}P-NMR. (.The error bars represent the standard deviation from the mean with n = 3)

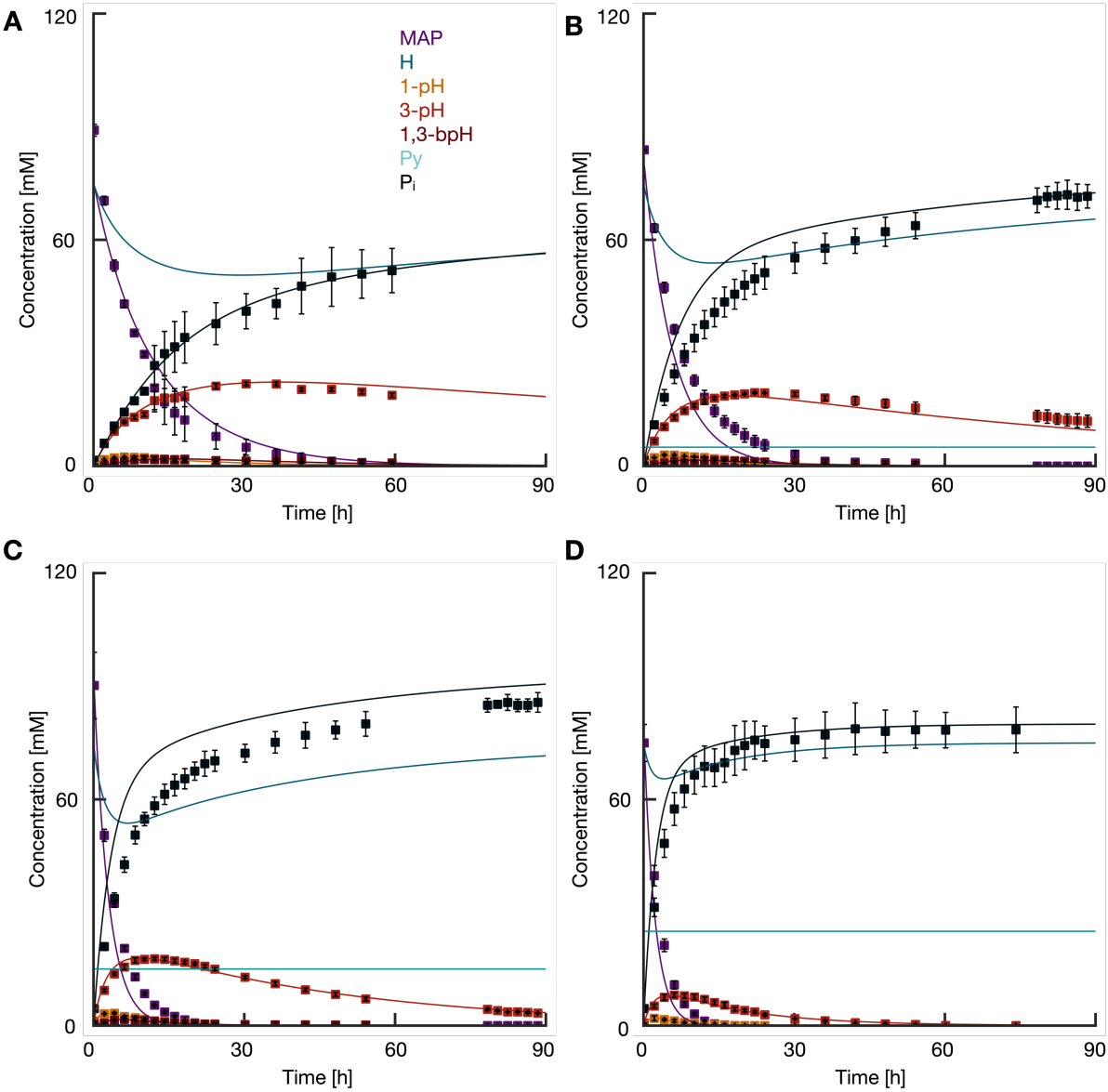

Figure S7 | | Concentration profiles (squares) and kinetic profiles (lines) of the phosphorylation cycle of Ac-GHG-OH with MAP at pH 7.5 and following pyridine concentrations **A.** 0, **B.** 5, **C.**15, and **D.** 25 mM recorded with ^{31}P-NMR. (The error bars represent the standard deviation from the mean with n = 3).

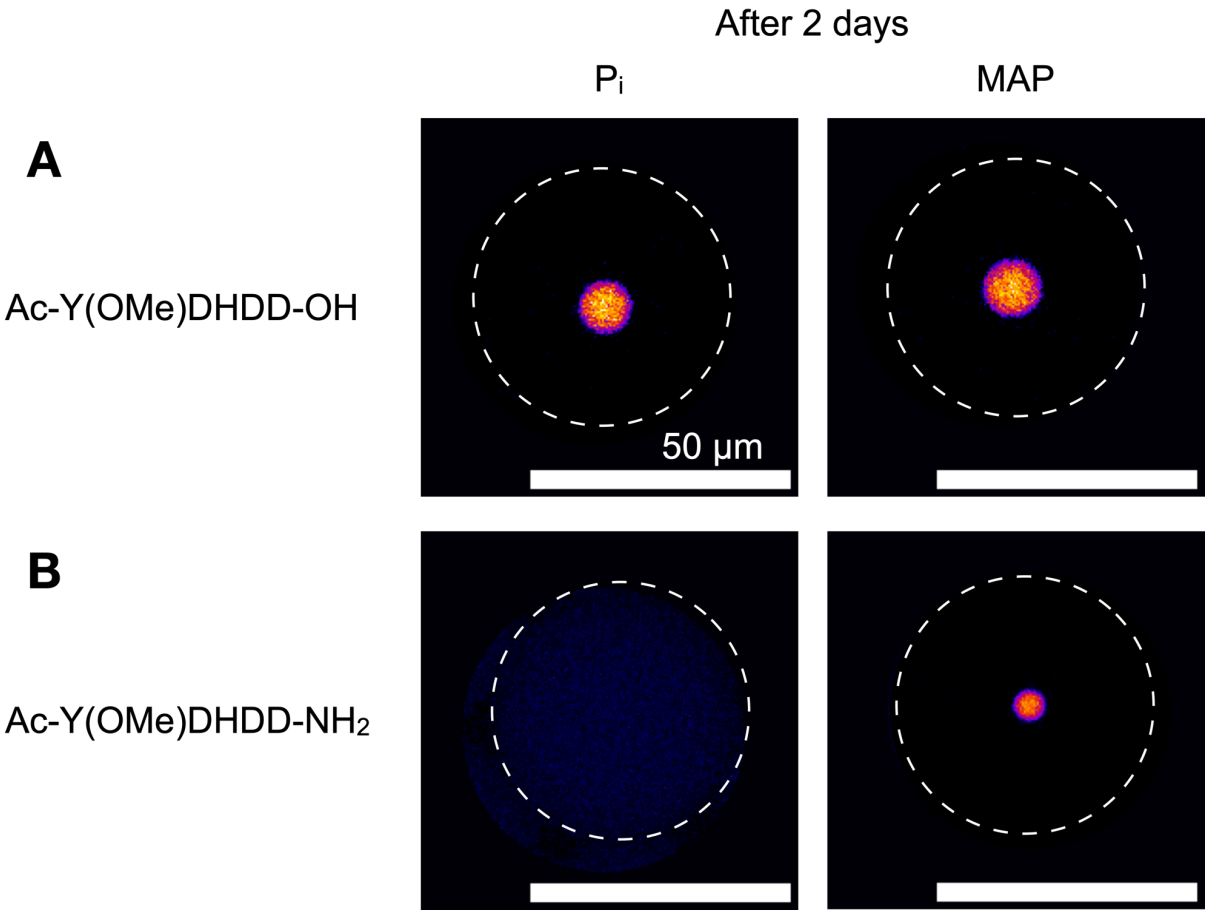

Figure S8 | Design of the peptide for complex coacervation formation. The dotted line represents the microreactor and the micrographs were recorded after 2 days. **A.** Ac-Y(OMe)DHDD-OH forms droplets with phosphate and MAP. **B.** Ac-Y(OMe)DHDD-NH_2 forms droplets only with MAP. (15 mM Ac-Y(OMe)DHDD-OH/20 mM Ac-Y(OMe)DHDD-NH_2, 12.5 mM P_i/MAP and 50 mM R_{30}in a 100 mM MOPS buffered solution at pH 7.5).

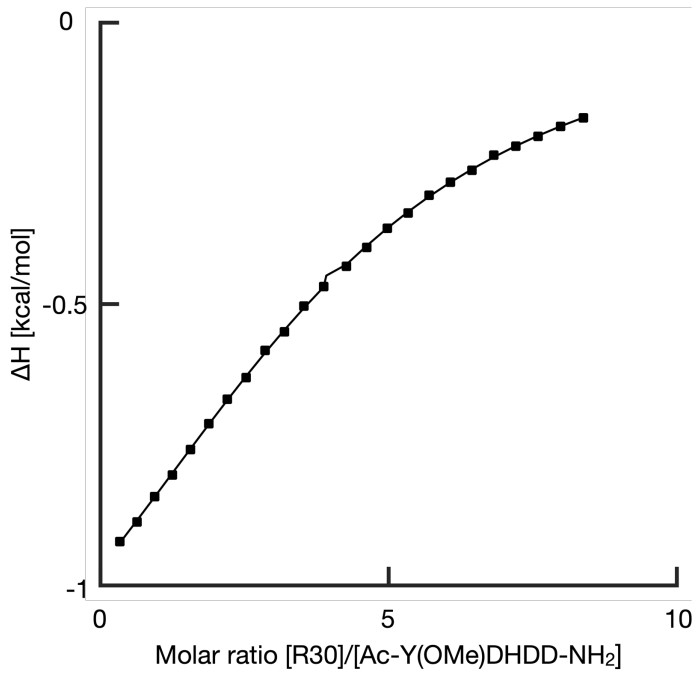

[Cell] [M] = 500e-6 (strand)
[Syringe] [M] = 10e-3
N(sites) = 4.42 ± 2.1e-2
K_D = 1.19e-3 ± 21.9e-6
ΔH (kcal/mol) = -1.17 ± e-2
Offset (kcal/mol) = 3.3e-3
ΔG (kcal/mol) = -3.99
-TΔS (kcal/mol) = -2.82

Figure S9 | ITC titration curve given in enthalpy change versus the molar ratio (Ac-Y(OMe)DHDD-NH_2/R_{30}).

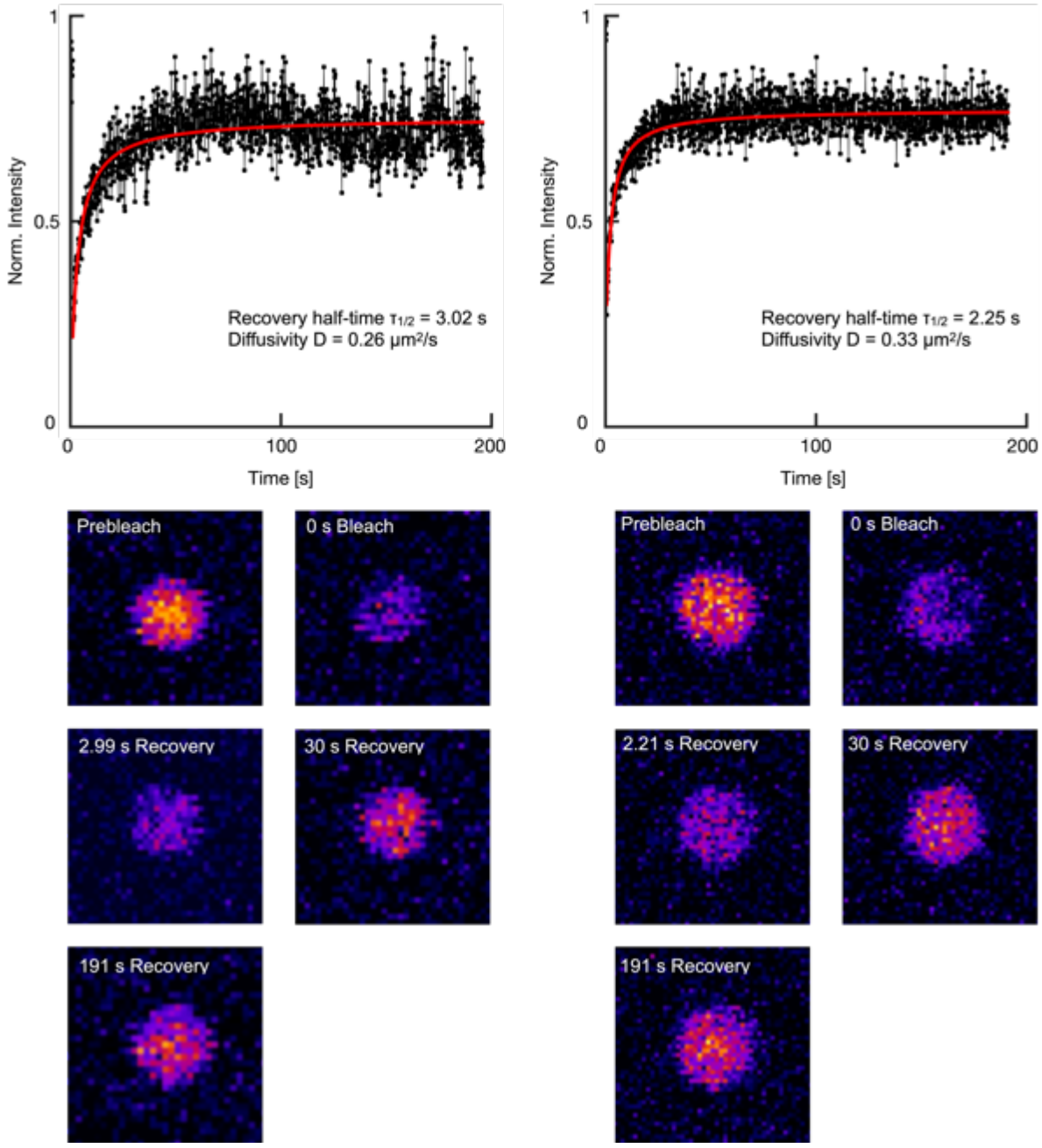

Figure S10 | Representative FRAP data 3 days after the start of the reaction cycle.

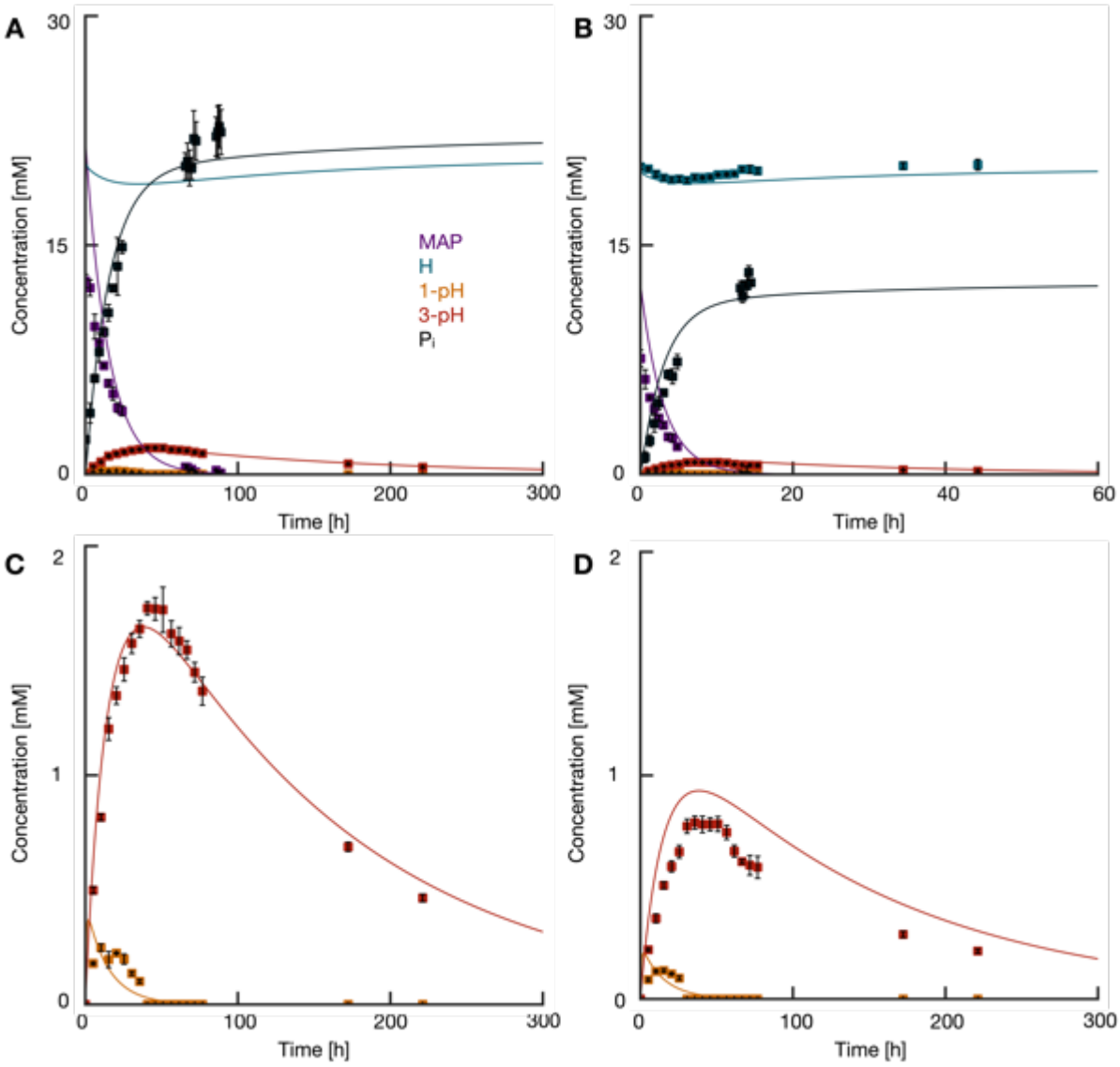

Figure S11 | Concentration profiles (squares) and kinetic profiles (lines) of the phosphorylation cycle of 20 mM Ac-Y(OMe)DHDD-NH_2 with **A.** and **C.** 25 mM and **B.** and **D.** 12.5 mM MAP in a 100 mM MOPS buffered solution at pH 7.5 followed with ^{31}P-NMR (MAP and P_i) and analytical HPLC (His, 1-pH, and 3-pH). **C.** and **D.** Magnification of the profiles 1- and 3-pH. (The error bars represent the standard deviation from the mean with n = 3).

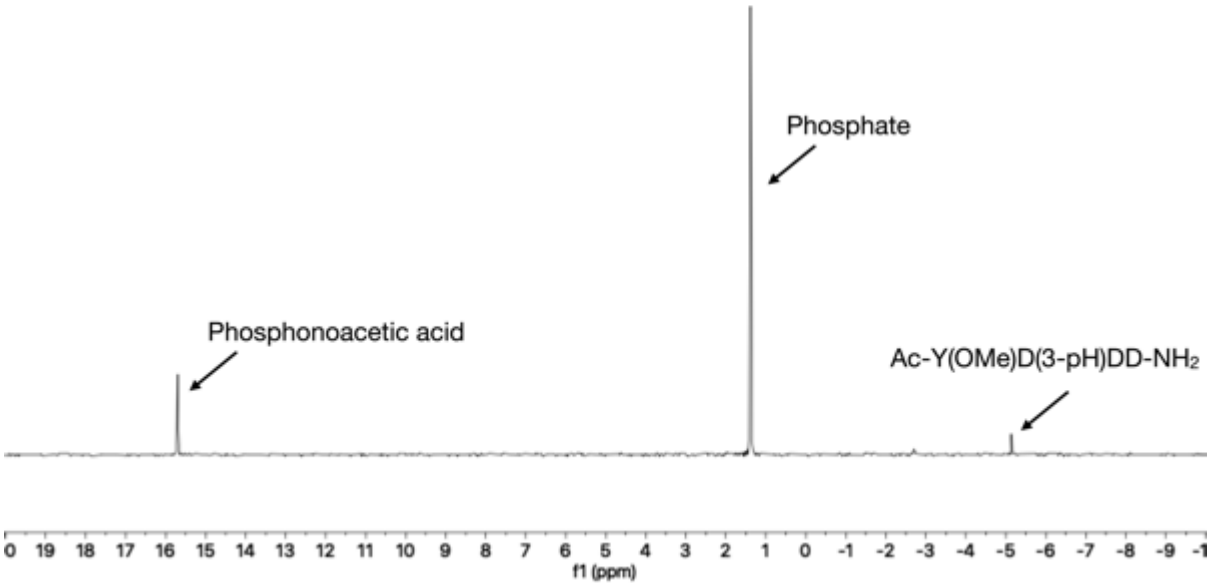

Figure S12 | Representative ^{31}P-NMR spectra of Ac-Y(OMe)D(3-pH)DD-NH_2 60 h after the start of the reaction (spectrum was recorded with 15 s relaxation delay and 256 scans).

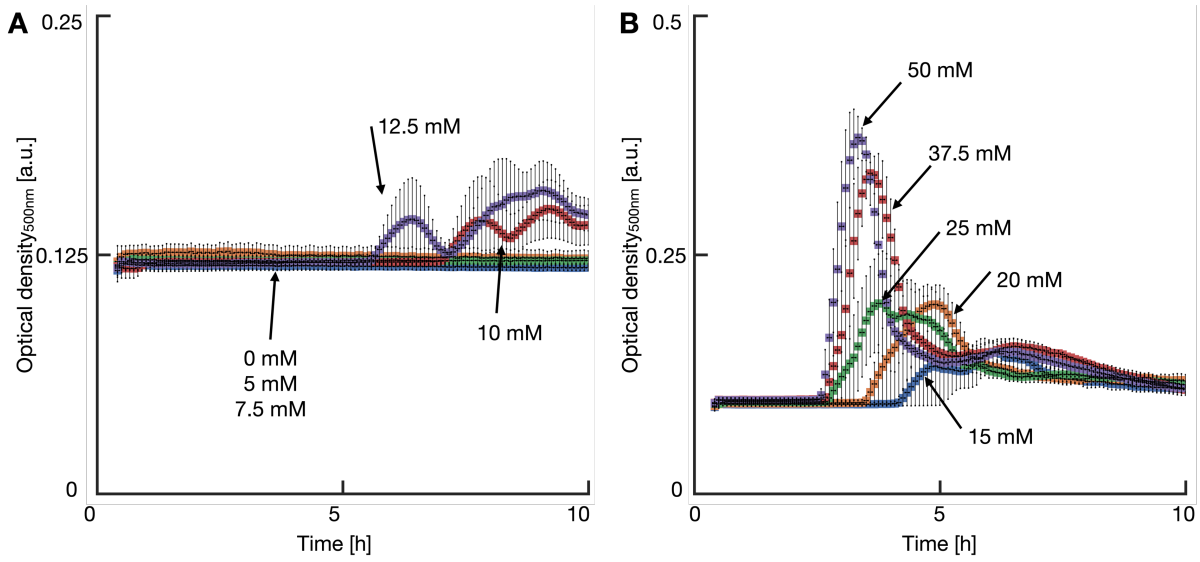

Figure S13 | Absorbance profiles to determine the lagtime and the maximum intensity dependent on fuel concentration. (20 mM peptide, 50 mM R30, 2.5% PEG8000, **A.** 0-5-7.5-10-12.5 mM **B.** 15-20-25-37.5-50 mM MAP, (12.5+x) mM Pi, (100-x) mM MOPs pH 7.5. (The error bars represent the standard deviation from the mean with n = 3).

References

[1] Y.-F. Wei, H. R. Matthews, *Methods in enzymology* **1991**, *200*, 388-414.
[2] C. Gibard, S. Bhowmik, M. Karki, E.-K. Kim, R. Krishnamurthy, *Nature Chemistry* **2018**, *10*, 212-217.
[3] T. J. Henderson, *Analytical Chemistry* **2002**, *74*, 191-198.
[4] R. Rigger, A. Rück, C. Hellriegel, R. Sauermoser, F. Morf, K. Breitruck, M. Obkircher, *Journal of AOAC International* **2017**, *100*, 1365-1375.
[5] D. C. Duffy, J. C. McDonald, O. J. Schueller, G. M. Whitesides, *Analytical chemistry* **1998**, *70*, 4974-4984.
[6] M. Weiss, J. P. Frohnmayer, L. T. Benk, B. Haller, J.-W. Janiesch, T. Heitkamp, M. Börsch, R. B. Lira, R. Dimova, R. Lipowsky, *Nature materials* **2018**, *17*, 89-96.
[7] T. W. Hofmann, S. Hänselmann, J.-W. Janiesch, A. Rademacher, C. H. Böhm, *Lab on a Chip* **2012**, *12*, 916-922.
[8] M. Kang, C. A. Day, A. K. Kenworthy, E. DiBenedetto, *Traffic* **2012**, *13*, 1589-1600.
[9] I. Alshareedah, T. Kaur, P. R. Banerjee, in *Methods in enzymology, Vol. 646*, Elsevier, **2021**, pp. 143-183.